JOURNAL OF COMPUTATIONAL PHYSICS 4, 475–498 (1969)

Spatial Differencing of the Transport Equation: Positivity vs. Accuracy[1]

K. D. LATHROP

Los Alamos Scientific Laboratory, University of California, Los Alamos, New Mexico

Received February 14, 1969

ABSTRACT

Positive spatial difference schemes for the Boltzmann equation are derived and compared in $x - y$ geometry. It is found that none of the positive schemes are as accurate as the most commonly used nonpositive scheme. A variable weighted difference scheme in which the weights are chosen depending on the space-angle mesh is shown to give results similar to those obtained with difference schemes based on the method of characteristics. A version of the variable weight scheme in which weights depend not only on the space-angle mesh but also on particle sources and fluxes is suggested as a means of obtaining the highest accuracy consistent with a positive difference scheme, but it is noted that such schemes are computationally more expensive than available corrective recipes used in conjunction with nonpositive schemes.

I. INTRODUCTION

One of the long-standing problems in the numerical solution of the finite difference form of the discrete ordinates equations is that the positivity of the solution cannot be guaranteed. In general, for a sufficiently fine spatial mesh, solutions are observed to be positive, but in many problems the angular flux, the angle-integrated flux or even the fission rate is found to be negative. This is frequently so because the range of cross section magnitudes or the size of the system considered is so large that a fine mesh is not possible.

In many cases the negative fluxes, while annoying, can be tolerated because they occur in regions in which fluxes are small and unimportant, but in an increasing number of situations, negative fluxes interfere with the solution process. In multidimensional solutions they slow the convergence rate of iterative processes, and sometimes cause the failure of acceleration procedures. In time dependent problems they cause instabilities, either in the transport solution or in associated

[1] Work performed under the auspices of the U.S. Atomic Energy Commission.

routines. In addition to these real difficulties, there are psychological problems associated with negative fluxes. The user who understands the transport equation and not the numerical solution procedure does know that there is no such thing as a negative angle-integrated flux, and rapidly becomes cynical about the effectiveness of the program which produces negative numbers.

For these reasons we have considered finite difference schemes which ensure positive solutions to the discrete ordinates equations. We do not mean corrective recipes, such as those in ANISN [1] or DTF-IV, [2] which, upon detection of a negative flux produced by the usual procedure, switch to another algorithm which prevents negative numbers; but rather finite difference schemes which guarantee that if the source and boundary fluxes are positive, then the calculated fluxes are positive. Because the most commonly used nonpositive scheme is both simple and accurate, we shall see that we must pay a premium, either in simplicity or accuracy, to enforce positivity. Here we have enumerated three desirable properties of a difference scheme: (1) it should be accurate in the sense that it has a small truncation error, (2) it should be simple, which we interpret to mean that it should involve a small number of numerical operations and should involve unknowns from within a single mesh cell, and (3) it should produce positive fluxes if the source and boundary fluxes are positive. To this list we add the requirements that (4) the scheme be conservative in the sense that a well defined relation exists among flows into and out of the cell and sources and absorptions in the cell and (5) the scheme is easily generalizable to all geometries.

We have investigated many different types of difference schemes. These fall into two categories: (1) characteristic schemes which are based on the known streaming properties of the transport equation, and (2) curve fitting schemes which are based on an assumed form of the distribution function. For the sake of completeness we here describe all of these schemes, drawing upon the earlier work of Carlson, Wendroff, Woods and the author. In all cases we restrict our description to (x, y) geometry in which we write the transport equation as

$$\mu \frac{\partial \psi}{\partial x} + \eta \frac{\partial \psi}{\partial y} + \sigma \psi(x, y, \mu, \eta) = S(x, y, \mu, \eta) \tag{1}$$

in which S is the source of particles, ψ is the angular flux (velocity times density), σ is the total macroscopic interaction cross section and μ and η are the x and y components (direction cosines) of the particle motion. Such an equation applies to each group of a multigroup approximation. We shall always assume that S is known although in almost every situation it depends on ψ. However, this dependence is usually found iteratively, and in each cycle of iteration, S is a known function. We always consider a single homogeneous cell of width Δx and height Δy so that $0 \leqslant x \leqslant \Delta x$ and $0 \leqslant y \leqslant \Delta y$, and we always assume that the angular

flux is known on two adjacent boundaries. Because we insist on 90° symmetry in our difference equations, we can always consider only one quadrant of direction cosines and determine other relations from symmetry. Therefore we always take μ and η to be positive and assume we know the left, $\psi_L(o, y, \mu, \eta)$, and bottom, $\psi_B(x, o, \mu, \eta)$, boundary fluxes. Our problem, then, is always to find the right, $\psi_R(\Delta x, y, \mu, \eta)$, and top, $\psi_T(x, \Delta y, \mu, \eta)$, fluxes and some flux $\psi_{\text{cell}}(\bar{x}, \bar{y}, \mu, \eta)$ within the cell from which S can be calculated.

By taking the two dimensional transport equation we encounter problems which do not occur in all one dimensional geometries. By restricting ourselves to (x, y) geometry, we avoid the problems of differencing the angular variable and deal only with spatial differencing of the transport equation. In this respect our work is preliminary because we have not fully come to grips with the simultaneous differencing of both space and angle. However, we shall see that certain schemes below are readily extended to curved geometries.

Our general plan is to describe characteristic schemes in Section II, curve fitting schemes in Section III, and certain numerical comparisons in Section IV. We summarize and discuss extensions of the work in Section V.

II. Difference Schemes Based on the Method of Characteristics

An assumption made in the derivation of the Boltzmann equation is that particles travel in straight lines between collisions. These straight lines are the characteristics of Eq. (1) which can be written

$$\frac{d\psi}{ds} + \sigma\psi = S \tag{2}$$

where the derivative is along the direction of motion. This equation forms the basis of several finite difference approximations to Eq. (1). We first describe a scheme that applies Eq. (2) directly.

A. *A Step Function Characteristic Scheme*

We integrate Eq. (2), writing

$$\psi = \psi_0 e^{-\sigma s} + \int_0^s S e^{-\sigma(s-s')}\, ds' \tag{3}$$

where ψ_0 is the flux on the boundary, s is the distance from the boundary to the point at which ψ is evaluated and s' is the point at which S is evaluated. If we assume that ψ_L and ψ_B are step functions in space, e.g., that $\psi_L(o, y, \mu, \eta)$ and $\psi_B(x, o, \mu, \eta)$

are functions of μ and η alone, and if we assume that S does not vary with x and y in the space cell, then we can integrate Eq. (3) to find

$$\begin{aligned} \psi_{\text{below}} &= S(\mu, \eta)(1 - e^{-\sigma y/\eta})/\sigma + \psi_B(\mu, \eta)\, e^{-\sigma y/\eta}, \\ \psi_{\text{above}} &= S(\mu, \eta)(1 - e^{-\sigma x/\mu})/\sigma + \psi_L(\mu, \eta)\, e^{-\sigma x/\mu}, \end{aligned} \tag{4}$$

depending on whether we are above or below the characteristic drawn through the lower left corner of the cell. These functions, of course, vary in the cell and along the right or top edges of the cell. We may, however, define the averages

$$\begin{aligned} \psi_R &= \int_0^{\Delta y} \psi(\Delta x, y, \mu, \eta)\, dy/\Delta y, \\ \psi_T &= \int_0^{\Delta x} \psi(x, \Delta y, \mu, \eta)\, dx/\Delta x, \\ \psi_{\text{cell}} &= \int_0^{\Delta x} \int_0^{\Delta y} \psi(x, y, \mu, \eta)\, dx\, dy/\Delta x\, \Delta y, \end{aligned} \tag{5}$$

and use Eq. (4) to evaluate these averages. The result of this process gives

$$\begin{aligned} \psi_R &= Q + (\psi_L - Q)(1 - \rho)\, e^{-\alpha} \qquad \rho < 1 \\ &\quad + (\psi_B - Q)\, \rho(1 - e^{-\alpha})/\alpha \\ \psi_T &= Q + (\psi_L - Q)(1 - e^{-\alpha})/\alpha \qquad \rho < 1 \end{aligned}$$

or

$$\begin{aligned} \psi_R &= Q + (\psi_B - Q)(1 - e^{-\beta})/\beta \qquad \rho > 1 \\ \psi_T &= Q + (\psi_L - Q)(1 - e^{-\beta})/(\rho\beta) \qquad \rho > 1 \\ &\quad + (\psi_B - Q)(1 - 1/\rho)\, e^{-\beta}, \end{aligned} \tag{6}$$

where the abbreviations which we use throughout are

$$\begin{aligned} Q &= S/\sigma \\ \alpha &= \sigma\Delta x/\mu \\ \beta &= \sigma\Delta y/\eta \\ \rho &= \alpha/\beta. \end{aligned} \tag{7}$$

Here, the value of ρ determines where the characteristic direction through the lower left corner intersects the top or right boundary of the cell. The derivation of these equations is given in somewhat more detail in Reference [3].

It is not hard to verify that the fluxes of Eq. (5) satisfy the relation

$$\mu \frac{(\psi_R - \psi_L)}{\Delta x} + \eta \frac{(\psi_T - \psi_B)}{\Delta y} + \sigma\psi_{\text{cell}} = S. \tag{8}$$

That is, the scheme is conservative in the sense noted in the introduction. Given that ψ_L, ψ_B and S are positive, the scheme is also easily shown to produce positive ψ_R and ψ_T. The truncation error, however, is something less than the second order error which is possible. It is possible to show that the relations of Eq. (6) have first order truncation error which depends on ρ, α, and β. The error is largest for large α and β, or for ρ near zero. The relations approach second order accuracy for ρ near one and small α and β. The scheme is also difficult to generalize; there are not many geometries in which it is so easy to integrate along the characteristics. This last difficulty is overcome by the next two characteristic schemes.

B. Wendroff's Characteristic Scheme

B. Wendroff [5] has suggested a scheme which accepts the generalized conservation form of the discretized transport equation as proposed by Carlson and Lathrop [6]. For (x, y) geometry this is simply Eq. (8) which he writes

$$\frac{\psi_P - \psi_Q}{\Delta s} + \sigma\psi = S, \tag{9}$$

by defining

$$\begin{aligned} \psi_P &= \Delta s(\mu\psi_R/\Delta x + \eta\psi_T/\Delta y), \\ \psi_Q &= \Delta s(\mu\psi_L/\Delta x + \eta\psi_B/\Delta y), \end{aligned} \tag{10}$$

and

$$\Delta s = 1/(\mu/\Delta x + \eta/\Delta y). \tag{11}$$

He then uses Eq. (3) with $\psi_0 = \psi_Q$ in the average

$$\frac{\int_0^{\Delta s} (S - \sigma\psi)\, ds}{\Delta s} \tag{12}$$

to find

$$\psi_P = \psi_Q e^{-\sigma\Delta s} + \int_0^{\Delta s} Se^{-\sigma(\Delta s - s')}\, ds'. \tag{13}$$

Although Wendroff assumed neither the constancy of σ or S across the cell, if this is done, Eq. (13) gives ($Q = S/\sigma$)

$$\psi_P = \psi_Q e^{-\sigma\Delta s} + Q(1 - e^{-\sigma\Delta s}). \tag{14}$$

In (x, y) geometry [or as noted by Wendroff in (x, t) space], if the characteristic defined by μ and η is drawn through the center of the mesh cell the projection of the characteristic on the (x, y) plane intercepts the line through the left and bottom cell boundary midpoints at a point Q and the line through the right and top cell boundary midpoints at a point P such that the distance between P and Q is the projection of Δs onto the (x, y) plane. Further ψ_Q can be regarded as the linear interpolation of ψ_L and ψ_B along the line joining the left, bottom cell midpoints and ψ_P as the similar linear interpolate of ψ_R and ψ_T. In other geometries, these identifications can be made only approximately.

Equation (14) is positive whenever ψ_L, ψ_B and S are positive, but we have as yet no way to determine ψ_R and ψ_T once ψ_P is known. Wendroff suggested, for a second order truncation error, the auxiliary relations

$$\psi_R + \psi_L = \psi_T + \psi_B \tag{15}$$

but with this assumption the positivity of ψ_R and ψ_T cannot be guaranteed. A positive method of partitioning ψ_P is discussed in the next section.

C. *The Woods-Carlson Characteristic Scheme*

D. Woods [7] derived Eq. (14) by first assuming

$$\psi = \frac{\psi_P + \psi_Q}{2}, \tag{16}$$

and then, in the resulting expression for ψ_P in terms of ψ_Q, replacing the fractions by the exponentials to which the fractions are the low-order approximations. Carlson [8] then suggested the following partitioning. Assume that ψ_R and ψ_T are a linear combination of ψ_L and ψ_B with undetermined coefficients:

$$\begin{aligned} \psi_R &= a_{11}\psi_L + a_{12}\psi_B + (1 - e^{-\sigma\Delta s})\, Q, \\ \psi_T &= a_{21}\psi_L + a_{22}\psi_B + (1 - e^{-\sigma\Delta s})\, Q. \end{aligned} \tag{17}$$

In this equation the form of the terms containing Q is chosen in analogy to Eq. (14). The undetermined coefficients are determined by requiring, first, that in the limit when all fluxes are equal Q, Eq. (17) is satisfied which gives

$$\begin{aligned} a_{11} + a_{12} &= e^{-\sigma\Delta s}, \\ a_{21} + a_{22} &= e^{-\sigma\Delta s}, \end{aligned} \tag{18}$$

and, second, that Eq. (14) is satisfied which gives

$$\begin{aligned} a_{11} + \rho a_{21} &= e^{-\sigma\Delta s}, \\ a_{12} + \rho a_{22} &= \rho e^{-\sigma\Delta s}. \end{aligned} \tag{19}$$

These two sets of equations represent only three independent equations. If we arbitrarily set $a_{22} = 0$, we have, with $\tau = e^{-\sigma\Delta s}$,

$$\begin{aligned} \psi_R &= (1 - \rho)\,\tau\psi_L + \tau\psi_B + (1 - \tau)\,Q, \\ \psi_T &= \tau\psi_L + (1 - \tau)\,Q, \end{aligned} \tag{20}$$

while if we set $a_{11} = 0$ we get

$$\begin{aligned} \psi_R &= \tau\psi_B + (1 - \tau)\,Q \\ \psi_T &= \tau/\rho\psi_L + (1 - 1/\rho)\,\tau\psi_B + (1 - \tau)\,Q. \end{aligned} \tag{21}$$

We can now use whichever relation has positive coefficients, i.e., Eq. (20) when $\rho < 1$ and Eq. (21) when $\rho > 1$. Note the similarity between these equations and those of the step function characteristic approach, Eq. (6).

The above scheme was tested in a variety of sample problems which are described in Section IV. In general, it gave results very similar to those obtained using the step function characteristic scheme. Because the Woods–Carlson scheme is simpler and easier to generalize to any geometry, it is preferable to the step function scheme. We describe in Section III a type of variable weight scheme which gives results very similar to these characteristic schemes.

D. Corner-Point Characteristic Schemes

Up to now we have been considering schemes which make use of only two boundary fluxes and one source in the cell. In such schemes the boundary flux, ψ_L say, is a single number representing the average amplitude of the flux along the left face of the cell [average as in Eq. (5)]. In corner-point schemes the angular flux is determined at all four corners of the cell and an estimate of the variation of the flux along a boundary can be made by linear interpolation.

A corner point scheme which uses the characteristic direction for interpolation is described by Gelbard *et. al.* [9]. In this scheme we denote the corner fluxes by ψ_{LB} for the left, bottom corner flux, ψ_{RT} for the right, top corner flux, etc. If the characteristic through the right, top corner is extended back through the cell, it intercepts either the left or bottom boundary. The flux at this point, ψ_Q say, can then be determined by linear interpolation. For our standard rectangle we have

$$\begin{aligned} \psi_Q &= \rho\psi_{LB} + (1 - \rho)\,\psi_{LT} && \rho < 1, \\ \psi_Q &= (1/\rho)\,\psi_{LB} + (1 - 1/\rho)\,\psi_{RB} && \rho > 1. \end{aligned} \tag{22}$$

This value of the boundary flux can be used in the integration along the characteristic direction to obtain the unknown flux at the top right corner, i.e.,

$$\psi_{RT} = \psi_Q e^{-\sigma \Delta s} + \int_0^{\Delta s} S e^{-\sigma(\Delta s - s')}\, ds', \tag{23}$$

where now Δs is given by

$$\begin{aligned} \Delta s &= \Delta x/\mu \qquad \rho < 1, \\ \Delta s &= \Delta y/\eta \qquad \rho > 1. \end{aligned} \tag{24}$$

In the scheme described by Gelbard, *et. al.*, use of exponentials was avoided by replacing ψ in Eq. (9) by $(\psi_P + \psi_Q)/2$ where now $\psi_P \equiv \psi_{RT}$. A similar recipe was used for the fluxes in the flux dependent portion of S.

This scheme, which allows linear variations along boundaries and along the characteristic, might have a second order truncation error, although the authors remark that it is less accurate than a known second order scheme described below. In the scheme, no use is made of a cell average flux and the conservation relation of Eq. (8) is not satisfied. In Reference 3, a ψ_{cell} was determined from Eq. (8), but there ψ_L was taken to be one-half $\psi_{LB} + \psi_{LT}$, etc. This in fact is erroneous, for as shown in the reference such a scheme gives incorrect values of ψ_{cell} as $\Delta x\, \Delta y \to 0$.

III. Difference Schemes Based on Assumed Forms of the Distribution Function

In the following paragraphs we describe difference schemes that are based on assuming a functional form of the flux in the cell. In these forms, unknown coefficients are determined by satisfying boundary conditions and the transport equation. When used to find solutions to integral equations this technique is sometimes called collocation.

In this section we show that the commonly used "diamond" scheme [10, 11] corresponds to assuming that ψ is a linear function of x and y in the cell, and that "weighted diamond" schemes correspond to performing weighted averages of a linear function for ψ. In the general weighted linear scheme we describe procedures for picking the weights such that the schemes are positive. We then show that the positive schemes have larger truncation error than the diamond scheme and suggest higher order schemes to compensate for this increased error.

A. *The Diamond Difference Scheme*

If we integrate Eq. (1) over the cell we find

$$\mu \int_0^{\Delta y} [\psi(\Delta x, y, \mu, \eta) - \psi(0, y, \mu, \eta)]\, dy + \eta \int_0^{\Delta x} [\psi(x, \Delta y, \mu, \eta) - \psi(x, 0, \mu, \eta)]\, dx + \sigma \int_0^{\Delta x} \int_0^{\Delta y} \psi(x, y, \mu, \eta)\, dx\, dy = \int_0^{\Delta x} \int_0^{\Delta y} S(x, y, \mu, \eta)\, dx\, dy. \tag{25}$$

By defining ψ_L, ψ_B and S_{cell} analogously to the definitions of ψ_R, ψ_T and ψ_{cell} in Eq. (5), we can substitute in Eq. (25) to produce

$$\mu \frac{(\psi_R - \psi_L)}{\Delta x} + \eta \frac{(\psi_T - \psi_B)}{\Delta y} + \sigma \psi_{\text{cell}} = S_{\text{cell}}, \tag{26}$$

as in Eq. (8). If now we assume that ψ is linear in x and y, e.g., that

$$\psi(x, y, \mu, \eta) = a_{00}(\mu, \eta) + a_{10}(\mu, \eta)\, x + a_{01}(\mu, \eta)\, y \tag{27}$$

then all the averages can be evaluated. We find

$$\begin{aligned} \psi_L &= a_{00} + a_{01}\, \Delta y/2 \\ \psi_R &= a_{00} + a_{10}\, \Delta x + a_{01}\, \Delta y/2 \\ \psi_B &= a_{00} + a_{10}\, \Delta x/2 \\ \psi_T &= a_{00} + a_{10}\, \Delta x/2 + a_{01}\, \Delta y \\ \psi_{\text{cell}} &= a_{00} + a_{10}\, \Delta x/2 + a_{01}\, \Delta y/2, \end{aligned} \tag{28}$$

and further that

$$\psi_L + \psi_R = \psi_B + \psi_T = 2\psi_{\text{cell}} \tag{29}$$

These are the diamond[2] difference scheme auxiliary relations usually used in conjunction with Eq. (26) to solve for ψ_R or ψ_T in terms of S, ψ_L and ψ_B. We see that ψ_L is the flux at the cell left edge midpoint. In fact each edge flux is the flux evaluated at the cell edge midpoint and the cell average flux is ψ of Eq. (27) evaluated at the cell midpoint. In such a scheme we have matched the boundary conditions at the left and bottom edge midpoints and satisfied the transport equation at the cell center to determine the three unknown coefficients in Eq. (27).

[2] The name diamond arises because the figure formed by joining the cell edge midpoints is a diamond.

From Eq. (28) [or (29)] and Eq. (26), the a_{ij} coefficients can be determined in terms of ψ_L, ψ_B and S. Then ψ_R and ψ_T can also be written in terms of these quantities. We have, with α and β defined in Eq. (7),

$$\begin{aligned} \psi_R &= [(\beta - \alpha - \alpha\beta/2)\,\psi_L + 2\alpha\psi_B + \alpha\beta Q]/D, \\ \psi_T &= [2\beta\psi_L + (\alpha - \beta - \alpha\beta/2)\,\psi_B + \alpha\beta Q]/D, \\ D &= \alpha + \beta + \alpha\beta/2. \end{aligned} \tag{30}$$

Here we encounter a surprising fact. Either the coefficient of ψ_L in the relation for ψ_R or that of ψ_B in the relation for ψ_T is negative. Thus, the diamond scheme, which is easily shown to have a second order truncation error, is nonpositive.

How might such a scheme be made positive? Instead of evaluating the boundary fluxes at the cell edge midpoints, we can gain additional freedom by evaluating them elsewhere along the edge and picking the point of evaluation to insure positivity. This notion is explored in the next section.

B. Weighted Difference Schemes

Suppose a weight function is introduced in the averages defined in Eq. (5). For example, with weight $w(x, y)$ we define

$$\psi_L = \frac{\int_0^{\Delta y} \psi(0, y, \mu, \eta)\, w(0, y)\, dy}{\int_0^{\Delta y} w(0, y)\, dy}, \tag{31}$$

and similarly for the other edge fluxes. The cell average flux is then

$$\psi_{\text{cell}} = \frac{\int_0^{\Delta x} \int_0^{\Delta y} \psi(x, y, \mu, \eta)\, w(x, y)\, dx\, dy}{\int_0^{\Delta x} \int_0^{\Delta y} w(x, y)\, dx\, dy}. \tag{32}$$

When we substitute Eq. (27) in these averages we find

$$\begin{aligned} \psi_L &= a_{00} + a_{01}\bar{y}_L \\ \psi_R &= a_{00} + a_{10}\,\Delta x + a_{01}\bar{y}_R \\ \psi_B &= a_{00} + a_{10}\bar{x}_B \\ \psi_T &= a_{00} + a_{10}\bar{x}_T + a_{01}\,\Delta y \\ \psi_{\text{cell}} &= a_{00} + a_{10}\langle x\rangle + a_{01}\langle y\rangle, \end{aligned} \tag{33}$$

where $\bar{y}_L$, $\bar{y}_R$ and $\langle y\rangle$ are the average (with respect to w) values of y on the left, on the right, or within the cell, respectively, and similar notation is used for the x

averages. If all the x averages are the same, say $\bar{x}$, and all the y averages are the same, say $\bar{y}$, (for example, if w is separable in x and y) then

$$(\bar{x}/\Delta x)\,\psi_R + (1 - \bar{x}/\Delta x)\,\psi_L = \psi_{\text{cell}}\,, \tag{34}$$

and

$$(\bar{y}/\Delta y)\,\psi_T + (1 - \bar{y}/\Delta y)\,\psi_B = \psi_{\text{cell}}\,. \tag{35}$$

These equations are the weighted diamond relations [12]. If $\bar{x} = \Delta x/2$, $\bar{y} = \Delta y/2$ we have Eq. (29) and if $\bar{x} = \Delta x$, $\bar{y} = \Delta y$ we have the step difference relations [12] in which $\psi_R = \psi_T = \psi_{\text{cell}}$. In terms of averages, this step scheme amounts to matching the left boundary condition at the top, left corner and the bottom boundary condition at the bottom, right corner while the transport equation is evaluated at the top, right corner. Here, the extrapolation is across the whole cell and the step scheme has first order truncation error in both variables.

In general, the truncation error of weighted difference schemes can be estimated by expanding the boundary fluxes in Taylor series. For example,

$$\begin{aligned}\psi_R &= \psi + (\Delta x - \bar{x})\,\frac{\partial\psi}{\partial x} + \frac{(\Delta x - \bar{x})^2}{2}\,\frac{\partial^2\psi}{\partial x^2}\cdots\\ \psi_L &= \psi - \bar{x}\,\frac{\partial\psi}{\partial x} + \frac{\bar{x}^2}{2}\,\frac{\partial^2\psi}{\partial x^2}\cdots\,,\end{aligned} \tag{36}$$

so that the derivative approximation

$$\frac{\psi_R - \psi_L}{\Delta x} = \frac{\partial\psi}{\partial x} + \frac{\Delta x - 2\bar{x}}{2}\,\frac{\partial^2\psi}{\partial x^2}\cdots\,, \tag{37}$$

is in error by terms of order Δx unless $\bar{x} = \Delta x/2$ in which case the expression is accurate to terms of order Δx^2. Similarly, the approximation to the y derivative is of second order only if $\bar{y} = \Delta y/2$.

If we solve Eq. (26) for ψ_R and ψ_T, using Eqs. (34) and (35), we find, with $\bar{x}/\Delta x = X$ and $\bar{y}/\Delta y = Y$,

$$\psi_R = \frac{[\beta - (1 - X)(\alpha\beta + \alpha/Y)]\,\psi_L + (\alpha/Y)\,\psi_B + \alpha\beta Q}{\beta + X(\alpha\beta + \alpha/Y)}\,, \tag{38}$$

$$\psi_T = \frac{(\beta/X)\,\psi_L + [\alpha - (1 - Y)(\alpha\beta + \beta/X)]\,\psi_B + \alpha\beta Q}{\alpha + Y(\alpha\beta + \beta/X)}\,. \tag{39}$$

For fixed values of X and Y, the coefficient of ψ_L in (38) or that of ψ_B in (39) can be negative. The exception to this statement is if $X = Y = 1$, so that of the weighted schemes with fixed coefficients, the step scheme is the only positive scheme.

C. Variable Weighted Schemes

While we cannot guarantee positivity with fixed weights, Carlson noted that it is possible, given α and β, to determine X and Y so that every coefficient in Eq. (38) and (39) is positive. In general we require

$$\beta > (1 - X)(\alpha\beta + \alpha/Y), \qquad \text{and} \qquad \alpha > (1 - Y)(\alpha\beta + \beta/X). \tag{40}$$

Further, if the solution for X or Y is less than $\frac{1}{2}$ we will take the value of $\frac{1}{2}$ because this minimizes the truncation error. For the same reason we want the allest values of X and Y that are greater than or equal $\frac{1}{2}$ and that satisfy Eq. (40). An acceptable approximate solution to this nonlinear optimization problem is given by

$$\begin{aligned} 1 - X' &= \frac{\beta}{\alpha(\beta + 2)} \qquad \text{with } X = \max(X', \tfrac{1}{2}), \\ 1 - Y' &= \frac{\alpha}{\beta(\alpha + 2)} \qquad \text{with } Y = \max(Y', \tfrac{1}{2}). \end{aligned} \tag{41}$$

The argument here is that if $Y = \frac{1}{2}$ in the first relation in (40), then $\alpha(\beta + 1/Y)$ is larger than for any other value of $Y > \frac{1}{2}$ and hence X is larger. But if X is larger than it would be for $Y = \frac{1}{2}$, it is safe to set $X = \frac{1}{2}$ in the second relation.

Note that if we had chosen X and Y such that the inequalities in Eq. (40) were equalities, then we would have no contribution from ψ_L in Eq. (38) or ψ_B in Eq. (39). In this respect, the variable weighted schemes are similar to characteristic schemes. In fact, in the test problems described below, the variable weight scheme described here gave results in close agreement with those of the two characteristic schemes tested.

The variable weighted scheme requires the calculation of Eq. (41) at each cell if Δx, Δy, μ, η, or σ is different than in other cells, but this is less time consuming than computing exponentials in characteristic schemes and is probably no more time consuming than testing the diamond scheme to see if a negative flux has been calculated. If storage permits, these factors can be precomputed. In this case, the computational effort of the variable weighted scheme is much less than other recipes to ensure positivity. Such a scheme has been implemented in the TWOTRAN (x, y) program [13].

Another, more accurate, version of the variable weighted scheme is possible. In Eqs. (38) and (39) we have guaranteed that the coefficient of ψ_L or ψ_B is positive, but if these fluxes are zero or small, or if the other fluxes or sources are large, this is unnecessary. What we really wish to ensure is the positivity of the numerator of these equations.

That is, we pick X and Y from

$$1 - X = \frac{\beta + \alpha(\psi_B + \beta Q)/\psi_L}{\alpha(\beta + 2)}, \tag{42}$$

$$1 - Y = \frac{\alpha + \beta(\psi_L + \alpha Q)/\psi_B}{\beta(\alpha + 2)}. \tag{43}$$

As in Eq. (41), if X or Y is less than $\frac{1}{2}$, a value of $\frac{1}{2}$ is used to minimize the truncation error. These relations depend on the fluxes and sources and cannot be precomputed. Such a scheme, however, allows the most accurate differencing consistent with positivity. This scheme has been implemented in the (r, z) version of the TWOTRAN [13] program where there are three weighting coefficients to pick, one for differencing the angular variable. As implied by this statement, the variable weight difference scheme is readily extended to other geometries.

We have several times noted that specific positive schemes have larger truncation error than the nonpositive diamond scheme. These observations are consistent both with the numerical results and a theorem due to Lax [14] which states if the coefficients of the difference schemes are non-negative, then the scheme is of first order accuracy except in special situations. Wendroff [5] calls these situations "uninteresting". We thus seem to have a choice between positivity and accuracy. We have tried to find the most accurate positive scheme by calculating coefficients like Eqs. (42) and (43). We now explore the possibility of using a higher order scheme, constrained to be positive and hence presumably less accurate than possible, but yet of greater accuracy than the schemes we have so far examined.

D. Higher Order Difference Schemes

A scheme that uses two edge fluxes and one cell flux (source) cannot be of more than second degree accuracy. That is, given the cell source and two boundary fluxes we can at most determine three unknown coefficients which are just enough for a linear functional dependence. If a second order functional dependence is used, three more conditions are needed to determine all the unknown coefficients. Because we already evaluate the cell edge fluxes, it would be possible to evaluate the sources at each of the four edges (and not in the center). For example, if we assume the second order functional

$$\psi = \sum_{i=0}^{2} \sum_{j=0}^{i} a_{ij} x^{i-j} y^j, \tag{44}$$

define ψ_L as this function at $(0, \Delta y/2)$, ψ_R as the function at $(\Delta x, \Delta y/2)$, ψ_B as ψ at $(\Delta x/2, 0)$, and ψ_T as ψ at $(\Delta x/2, \Delta y)$, we obtain two equations (only two because

ψ_T and ψ_R are unknown) for the a_{ij}. We then substitute Eq. (44) in Eq. (1) and evaluate the result at the same four points. Interestingly, solving these six equations gives Eq. (30) with Q replaced by

$$(Q_R + Q_L)/2 + (Q_R + Q_L - Q_B - Q_T)/\beta, \tag{45}$$

in the equation for ψ_R and by

$$(Q_T + Q_B)/2 + (Q_T + Q_B - Q_R - Q_L)/\alpha, \tag{46}$$

in the equation for ψ_L. If each of the four sources is equal Q, then these equations reduce to Q. This scheme is very similar to the diamond scheme but it makes use of the variation of the source across the cell and is presumably a more accurate scheme. Like the diamond scheme it is not positive.

However, it seems to be possible to use this procedure to produce schemes which are constrained to produce positive fluxes. Presumably these schemes would involve choosing parameters in much the same way as in the variable weighted schemes, but could still yield, say, a second order scheme. This seems preferable to doubling the number of mesh intervals in a first order scheme, thereby halving the error. The conjecture here is that the non-linear nature of equations like (42) and (43) will permit circumvention of the Lax theorem.

Interesting applications are possible if the coefficients of an assumed functional form are determined. Most system descriptions consist of blocks of homogeneous composition. In such a block of I by J intervals a polynomial could be assumed of just sufficient degree to match J left boundary conditions, I bottom boundary conditions, and satisfy the transport equation at $I \times J$ fixed interior points. This determines a matrix equation which, for a given block, can be solved once and for all for the a_{ij}. Then any interior or boundary flux is easily constructed. This makes feasible the concept of line deletion, i.e., changing the number of intervals in passing from one block to another, because the appropriate interpolating polynomial is constructed by this procedure. Provided block sizes are limited so that the matrices involved can be easily inverted, such a high order scheme seems attractive.

IV. Numerical Comparisons of Difference Schemes

As an illustration of the type of flux behavior that is encountered when using the diamond scheme, we plot in Fig. 1 the angle-integrated flux obtained when a crude model is used to describe a reactor. The flux here is the horizontal traverse along the top edge ($y = 20.5$ cm) of a 25×25 cm assembly. Within this uranium assembly there is a core ($5.0 \leqslant x \leqslant 10.0$, $5.0 \leqslant y \leqslant 10.0$) of enriched uranium, but a fission source is present throughout. In the figure we show only the first

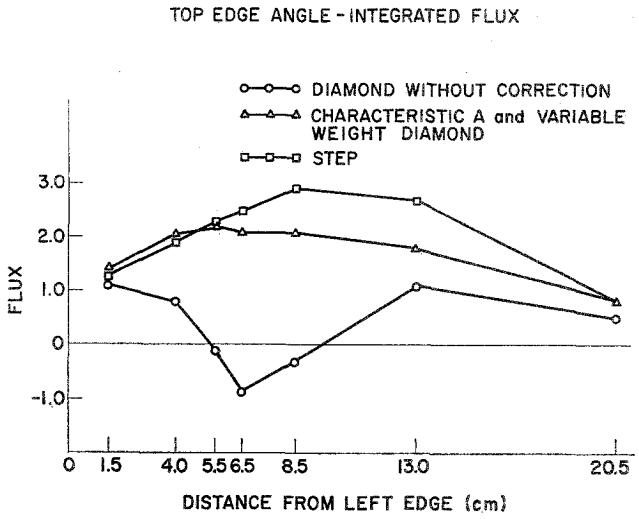

FIG. 1. Angle-integrated flux along the top edge of a bare rectangular reactor.

group (highest energy) fluxes. A total of 49 mesh cells were used to describe this system. While this description is crude, this simple test problem faithfully mirrors the situation that occurs repeatedly in design calculations: because of storage limitations or the desire to run a large number of survey calculations, the space mesh is crude. In this calculation the diamond scheme clearly gives an erroneous estimate of the local (e.g., $5.5 < x < 8.5$) reaction rates. The positive schemes plotted for comparison do indeed correct the negative fluxes. Shown on the figure are fluxes obtained using the characteristic scheme of Eq. (6) (labeled characteristic A), the step scheme [Eqs. (38) and (39) with $X = Y = 1$], and the variable weight scheme [Eq. (41) for X and Y used in Eqs. (38) and (39)]. The fluxes obtained with the Woods–Carlson scheme are so close to the Characteristic A results that they are omitted for clarity. Despite the local negative fluxes, the global reaction rates (e.g., system integrated fission rates) obtained with the diamond scheme are more accurate (compared to calculations with greatly refined meshes) than those obtained with the positive schemes. In general, the positive schemes force more particles to leave a finite system than does the diamond scheme. Hence, when fission is present the reactivity is underestimated. In shielding situations, an overestimate of the emerging flux is obtained when positive schemes are used.

The above illustration indicates the qualitative nature of the schemes. To precisely estimate the accuracy of the various schemes, we devised several simple, one-group test problems. In each of these problems we used a uniform mesh in x

and y and varied the size of Δx and Δy. Such calculations were performed for a variety of secondaries ratios ($c = \sigma_s/\sigma_t$) ranging from $c = 0$ (pure absorber) to $c = 0.99$. In each problem we tabulated the total number of absorptions in the system. All problems were run with vacuum boundary conditions, $\sigma_t = 1.0$ and S_4 quadrature defined by the (μ, η) pairs: (0.30163878, 0.30163878), (0.90444905, 0.30163878), (0.30163878, 0.90444905).

All the test problems were calculated using the step characteristic scheme [Eq. (6), labeled characteristic A in the figures], the Woods–Carlson scheme [Eqs. (20) and (21), labeled characteristic B in the figures], the step scheme [Eqs. (38) and (39) with $X = Y = 1$], and a version of the diamond scheme. This version, labeled DIAMF in the figures, applied Eq. (30) but did not allow ψ_R or ψ_T to becomes less than $\alpha\beta Q/D$. That is, the extrapolated fluxes were allowed to become no smaller than if both incoming boundary fluxes were zero. This is a version of a "fix-up" scheme in which continuous testing is required to determine if extrapolated fluxes fall below the limiting value. If they do, they are assigned the limiting value and the cell flux is recomputed from the conservation relation, Eq. (26). While such a scheme guarantees the positivity of the edge fluxes, it does not ensure a positive cell flux. For example, whenever an edge flux is limited, more particles are forced out of the cell than would otherwise have been, and the cell flux is consequently lowered. For this reason this scheme has been abandoned. In most of the test problems this limited version gave results in close agreement with the pure diamond scheme.

The first test problem consisted of uniform, isotropic, 1×1 mean free path square source located in a homogeneous square two mean free paths on a side. The total absorption rate was computed for $c = 0.0$, 0.3, 0.6, 0.9, and 0.99, for 4, 8, 16, and 32 intervals per mean free path. These results are listed in Table I. The problem geometry and plots of the results are displayed, for $c = 0.0$, in Fig. 2, and for $c = 0.99$ in Fig. 3. In these problems, the twelve-angle S_4 quadrature was used as a standard, but some higher order results are plotted in the figures.

We note that in all cases the accuracy of the step scheme is very poor, and the convergence rate is slow. In the case of the pure absorber the properties of the characteristic schemes and the DIAMF scheme are markedly similar, while in the scattering medium the two characteristic schemes give very similar results, but are much slower to converge than the DIAMF scheme. Two reasons for this behavior can be given. First, because we are comparing absorption rates, the interaction of the angular quadrature with the difference scheme has not been isolated. The step characteristic scheme has been shown [3] to give better angle-integrated fluxes in a pure absorber than the pure diamond scheme, probably for this reason. Second, in the case of the DIAMF scheme in a pure absorber with a small number of intervals, the limiting action of the scheme tends to increase leakage and decrease absorption.

TABLE I

FRACTION OF PARTICLES ABSORBED: 1×1 SQUARE S_4 ANGULAR QUADRATURE

Number of intervals per mean free path	Step	Step characteristic (A)	Woods characteristic (B)	DIAMF
$c = 0.0$				
4	.70880	.73268	.73463	.73244
8	.72217	.73617	.73728	.73630
16	.73038	.73791	.73849	.73814
32	.73487	.73876	.73906	.73892
64				.73927
$c = 0.3$				
4	.62002	.64259	.64370	.64813
8	.63316	.64676	.64754	.65060
16	.64133	.64873	.64917	.65094
32	.64583	.64968	.64991	.65069
$c = 0.6$				
4	.46984	.48861	.48865	.49851
8	.48138	.49315	.49346	.49801
16	.48868	.49521	.49544	.49732
32	.49274	.49618	.49630	.49715
$c = 0.9$				
4	.17256	.18042	.17986	.18608
8	.17780	.18306	.18296	.18544
16	.18120	.18421	.18421	.18529
32	.18313	.18473	.18474	.18524
$c = 0.99$				
4	.02002	.02099	.02089	.02171
8	.02069	.02135	.02133	.02166
16	.02112	.02151	.02150	.02165
32	.02137	.02158	.02158	.02165

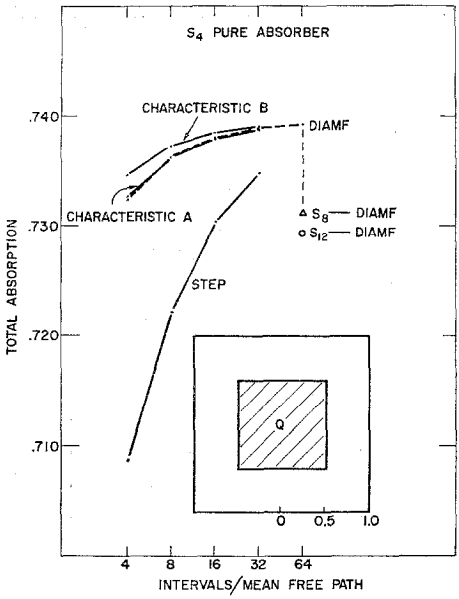

FIG. 2. Absorption fraction for a square unit source in a square. $c = 0.0$.

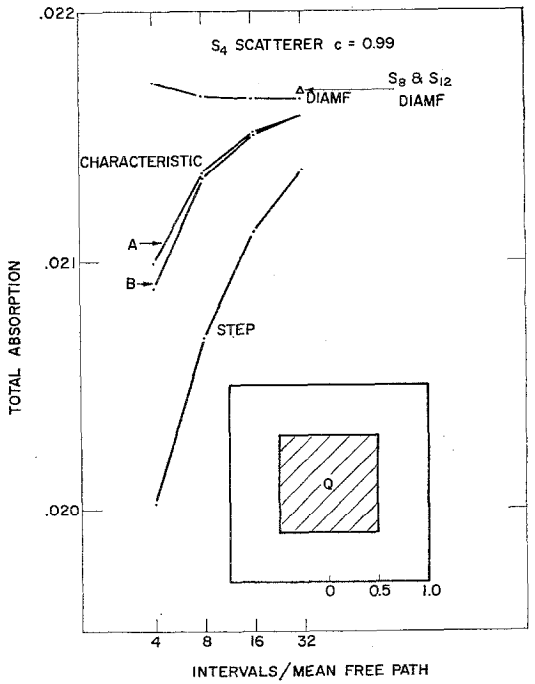

FIG. 3. Absorption fraction for a square unit source in a square. $c = 0.99$.

In the second test problem, a square source in a 2×8 mean free path rectangle, similar results were obtained. These are listed in Table II and plotted in Figs. 4 and 5. In this problem, the Woods–Carlson scheme seems to converge somewhat faster than the step characteristic scheme.

TABLE II

FRACTION OF PARTICLES ABSORBED:
2×8 RECTANGLE WITH $\Delta x = \Delta y$ S_4 ANGULAR QUADRATURE

Number of intervals per mean free path	Step	Step characteristic (A)	Woods characteristic (B)	DIAMF
$c = 0.0$				
4	.81735	.82777	.83242	.82686
8	.82514	.83149	.83404	.83246
16	.83009	.83360	.83494	.83451
32	.83289	.83473	.83542	.83531
$c = 0.3$				
4	.74848	.75818	.76286	.76195
8	.75631	.76240	.76502	.76639
16	.76129	.76470	.76609	.76723
32	.76411	.76591	.76662	.76718
$c = 0.6$				
4	.61500	.62319	.62754	.63236
8	.62243	.62789	.63042	.63307
16	.62721	.63033	.63170	.63293
32	.62991	.63158	.63229	.63287
$c = 0.9$				
4	.26925	.27336	.27572	.28022
8	.27372	.27679	.27826	.28024
16	.27664	.27848	.27929	.28020
32	.27831	.27932	.27974	.28017
$c = 0.99$				
4	.034527	.035121	.035457	.036200
8	.035213	.035682	.035898	.036231
16	.035667	.035953	.036074	.036228
32	.035929	.036085	.036149	.036222

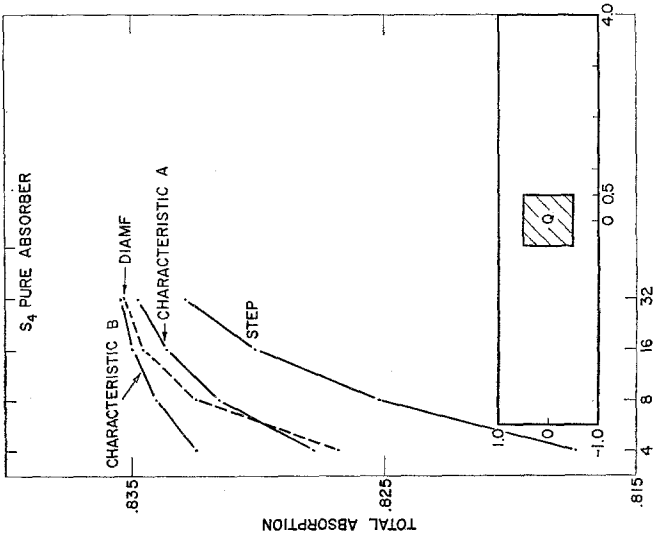

FIG. 4. Absorption fraction for a square unit source in a rectangle. $c = 0.0$.

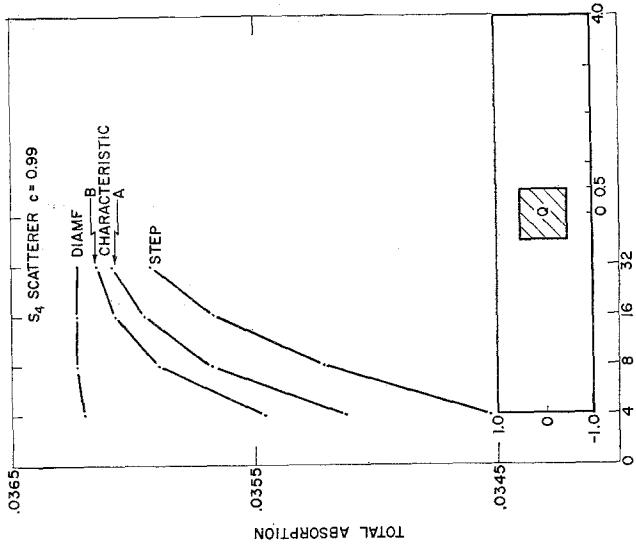

FIG. 5. Absorption fraction for a square unit source in a rectangle. $c = 0.99$.

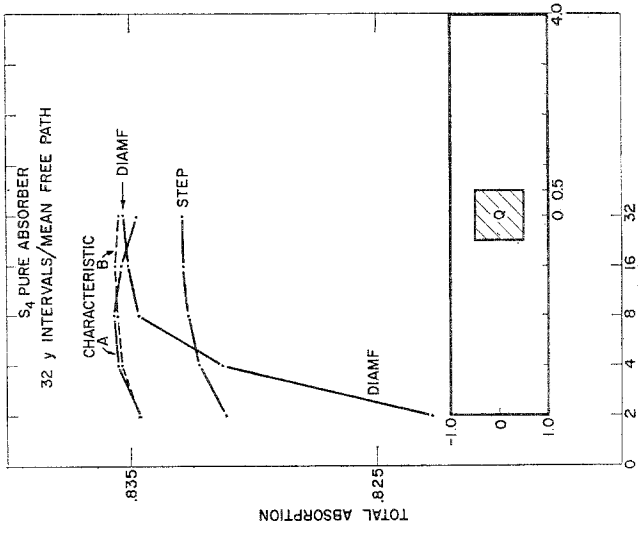

FIG. 6. Absorption fraction for a square unit source in a rectangle with $\Delta x \neq \Delta y$. $c = 0.0$.

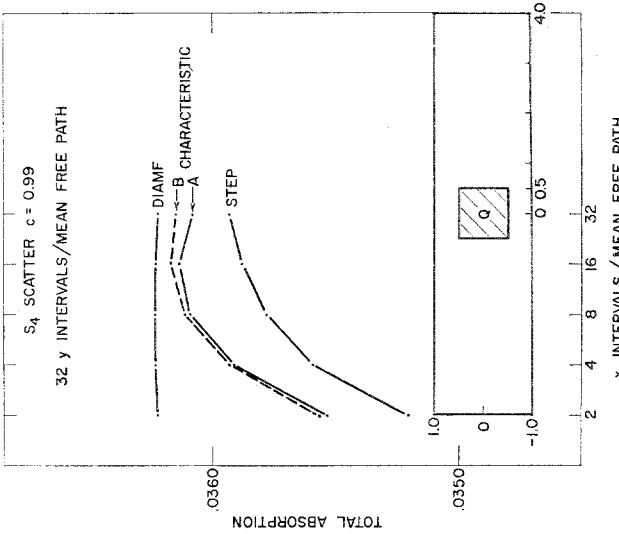

FIG. 7. Absorption fraction for a square unit source in a rectangle with $\Delta x \neq \Delta y$. $c = 0.99$.

TABLE III

FRACTION OF PARTICLES ABSORBED: 2×8 RECTANGLE WITH $\Delta x \neq \Delta y$
$32y$ INTERVALS PER MEAN FREE PATH S_4 ANGULAR QUADRATURE

Number of x intervals per mean free path	Step	Step characteristic (A)	Woods characteristic (B)	DIAMF	Variable weight diamond
$c = 0.0$					
2	.83113	.83454	.83460	.82277	.83463
4	.83223	.83543	.83531	.83125	.83558
8	.83265	.83563	.83554	.83465	.83589
16	.83282	.83533	.83564	.83510	.83562
32	.83289	.83473	.83542	.83531	.83497
$c = 0.3$					
2	.76160	.76510	.76523	.75511	.76519
4	.76311	.76639	.76632	.76373	.76654
8	.76373	.76677	.76671	.76651	.76704
16	.76399	.76653	.76686	.76710	.76682
32	.76411	.76591	.76662	.76718	.76615
$c = 0.6$					
2	.62617	.62960	.62983	.62147	.62969
4	.62833	.63156	.63158	.63118	.63171
8	.62928	.63229	.63229	.63267	.63255
16	.62971	.63218	.63252	.63286	.63247
32	.62991	.63158	.63229	.63287	.63181
$c = 0.9$					
2	.27436	.27649	.27670	.27894	.27654
4	.27651	.27858	.27868	.28004	.27867
8	.27756	.27952	.27958	.28022	.27967
16	.27807	.27966	.27988	.28021	.27984
32	.27831	.27932	.27974	.28017	.27945
$c = .99$					
2	.03520	.03553	.03556	.03622	.03553
4	.03559	.03591	.03593	.03623	.03592
8	.03578	.03609	.03611	.03623	.03612
16	.03588	.03613	.03617	.03623	.03616
32	.03593	.03608	.03615	.03622	.03610

In both of the above test problems, $\Delta x = \Delta y$. In the third test problem, the number of y intervals per mean free path was fixed and the number of x intervals per mean free path was varied for the 1×1 square source in the 2×8 rectangle. These results are listed in Table III and plotted in Figs. 6 and 7. Here again, the behavior of the various schemes is similar, but the unsatisfactory effect of the DIAMF limit is clearly evident (Fig. 5) in the pure absorber. For this problem we also computed the absorption rate using the variable weight scheme [Eq. (41) for X and Y used in Eqs. (38) and (39)]. These numbers are listed in Table III but are not shown in the Figures. When plotted, these numbers fall almost on top of the characteristic schemes results. Similar correspondence was noted in flux comparisons in other problems, some so crudely defined that the fission rates were negative with the pure diamond scheme.

In the results of Figs. 6 and 7 it does not appear that the results are converging toward the same total absorption. Here, it must be remembered that these results are for changing sizes of Δx with Δy fixed.

It has been our general observation that the characteristic and variable weighted diamond schemes produce much smoother angle-integrated fluxes than the diamond scheme. It seems likely that the diamond scheme angle-integrated fluxes, even when positive, are combinations of positive and negative angular fluxes. Typically, the angle-integrated flux produced by the diamond scheme displays jagged oscillations which are smoothed by the other schemes. A byproduct of this smoothness is the faster convergence of the iterative solutions.

V. Summary and Conclusions

We have examined many different schemes for spatial differencing of the transport equation and seen that all of the positive schemes are less accurate than the nonpositive diamond scheme. Of the positive schemes we feel that the variable weighted scheme is the most attractive, both because it is simpler than positive characteristic schemes and because it can be made as accurate as is possible for the system being considered. Thus when positive, relatively smoothly varying fluxes are desired, we suggest that such schemes be used.

However, when global accuracy is desired, we conclude that the fixup schemes, which ensure a minimum change from the diamond scheme, are to be preferred to the strictly positive schemes. This conclusion is based partly on the desire for accuracy and partly on the relative ease of implementation. While in the fixup algorithms (switch-to-the-step-scheme in ANISN [1] or set-offending-flux-to-zero-and-recompute-remaining-fluxes in DTF-IV [2]) continuous testing of the source (to prevent fixup if it is negative) and three extrapolated fluxes is required, this is generally faster than performing the additional arithmetic operations implied

by three (general geometry) equations like Eqs. (42) and (43). Also, while it is true that the positive schemes converge more swiftly, this advantage is offset by the larger number of space cells usually required for the same accuracy.

Despite the advantages of the fixup schemes we feel that if a positive scheme with *second* order truncation error could be derived it would justify additional computational effort. We have suggested that higher order positive schemes may be possible at the expense of a more complicated module, that is, if more boundary conditions and sources are used in each cell. It is possible that such difference schemes can be derived from a suitably constrained variational principle. The variational work of Kaplan [15] should be most instructive in this regard and should also be most useful when the problem of simultaneous space-angle differencing is considered.

References

1. W. W. Engle, Jr., "A Users Manual for ANISN," USAEC Report K-1693, Union Carbide Corporation (March 1967).
2. K. D. Lathrop, "DTF-IV, A FORTRAN-IV Program for Solving the Multigroup Transport Equation with Anisotropic Scattering," USAEC Report LA-3373, Los Alamos Scientific Laboratory (November 1965).
3. K. D. Lathrop, "Spatial Differencing of the Two-Dimensional Transport Equation," Report GA-8746, Gulf General Atomic (July 1968).
4. K. D. Lathrop, "New Spatial Difference Equations for Two-Dimensional Transport." *Trans. Am. Nucl. Soc.* **11**, 531 (1968).
5. B. Wendroff, "A Difference Scheme for Radiative Transfer," *J. Comput. Physics.* **2**, 211 (1969).
6. B. G. Carlson and K. D. Lathrop, Transport theory—The method of discrete ordinates, *in* "Computing Methods in Reactor Physics," Chap. 3, Gordon and Breach, New York (1968).
7. B. G. Carlson, "Transport Theory: Formulations and Solutions by Finite Difference Methods," Report LA-4016, Los Alamos Scientific Laboratory (September 1968).
8. B. G. Carlson, private communication, August 1968.
9. E. M. Gelbard, J. A. Davis, and L. A. Hageman, "Solution of the Discrete Ordinate Equation in One and Two Dimensions," USAEC Report WAPD-T-2028, Bettis Atomic Power Laboratory (July 1967).
10. B. G. Carlson, Numerical formulation and solution of neutron transport problems, *in* "Proceedings IBM Scientific Computing Symposium Large-Scale Problems in Physics." IBM, New York (1965).
11. B. G. Carlson and K. D. Lathrop, *op. cit.*
12. K. D. Lathrop and B. G. Carlson, *J. Comput. Phys.* **2**, 173 (1966).
13. K. D. Lathrop, "TWOTRAN, A FORTRAN Program for Two Dimensional Transport," Report GA-8747, Gulf General Atomic (July 1968).
14. P. D. Lax, *Commun. Pure Appl. Math.* **14**, 497 (1961).
15. S. Kaplan, *Nucl. Sci. Eng.* **34**, 76 (1968).